Spin dynamics in a two-dimensional disordered $S=\frac{1}{2}$ Heisenberg paramagnet from ^{63}Cu NQR relaxation in Zn-doped La_2CuO_4

P. Carretta, A. Rigamonti, and R. Sala
Department of Physics ''A. Volta,'' Unitá INFM and Sezione INFN di Pavia, Via Bassi, 6, 27100-I Pavia, Italy
(Received 1 April 1996; revised manuscript received 10 September 1996)

^{63}Cu NQR T_1 and T_2 relaxation measurements in $La_2Cu_{1-x}Zn_xO_4$, for $0\leqslant x\leqslant 0.11$ and in the temperature range $T_N\leqslant T\leqslant 900$ K, are presented. The results are used to derive insights into the Cu^{2+} correlated spin dynamics in the paramagnetic phase of the $S=\frac{1}{2}$ two-dimensional (2D) Heisenberg (H) antiferromagnets (AF), and into the disorder effects associated with the spin vacancy due to Zn^{2+} $(S=0)$ for Cu^{2+} substitution. In particular, by using scaling arguments for the static generalized susceptibility, $\chi(\vec{q},0)$, and for the decay rate, $\Gamma_{\vec{q}}$, of the normal excitations, T_2 and T_1 are related to the in-plane correlation length $\xi_{2D}(x,T)$ and its dependence on temperature and Zn doping, x, is extracted. The experimental findings are analyzed in light of the quantum critical and renormalized classical behaviors for ξ_{2D} predicted by recent theories for $S=1/2$ HAF on square lattices. It is shown that up to $T\simeq 900$ K, ξ_{2D} is consistent with the assumption of a renormalized classical regime, in agreement with recent neutron scattering results and at variance with previous interpretations of the NQR data. It is discussed how Zn affects ξ_{2D} through the modification in the spin stiffness and comparison with the disorder induced by itinerant extra holes is made. [S0163-1829(97)05806-2]

I. INTRODUCTION

La_2CuO_4, besides being the parent of high temperature superconductors, can be considered as a prototype for the investigation of quantum $S=1/2$ magnetism in planar Heisenberg antiferromagnets (2D-QHAF). Also in view of the efforts to clarify the mechanisms underlying high temperature superconductivity, La_2CuO_4 and related systems have attracted a great deal of theoretical and experimental interest.[1] From early neutron scattering studies[2] an exponential temperature dependence of the magnetic correlation length for $T>T_N$ was observed and interpreted as the 2D critical behavior towards an ordered state at $T_N^{2D}=0$ K, as expected for 2D Heisenberg systems. The transition to the AF ordered state is driven at $T_N\simeq 315$ K by the crossover, in a narrow temperature range, to a 3D behavior associated to the small interplane exchange coupling $J'\simeq 10^{-5}J$, whereas the intraplane exchange interaction is $J\simeq 1500$ K. Well above T_N recent theories for critical phenomena in 2D-QHAF (Refs. 3 and 4) predict that La_2CuO_4 is in the renormalized classical (RC) regime, in which the spin wave stiffness constant ρ_s and the spin wave velocity c_{sw} are renormalized by quantum fluctuations with respect to the correspondent mean field approximation (MFA) values.

In the RC regime, in La_2CuO_4, one expects[4] for the in-plane magnetic correlation length

$$\xi_{2D}\simeq \frac{\hbar c_{sw}}{16\pi k_B\rho_s}e^{2\pi\rho_s/T}\left(1-0.5\frac{T}{2\pi\rho_s}\right)$$
$$=0.493ae^{1.15J/T}\left[1-0.43\frac{T}{J}+O\left(\frac{T}{J}\right)^2\right], \qquad (1)$$

where a is the lattice unit and where the spin stiffness has been written $\rho_s=1.15J/2\pi$, while $c_{sw}=1.18\sqrt{2}Jk_Ba/\hbar$.

At temperatures higher than about $2\rho_s\simeq 600$ K, instead of going towards the classical limit $T\gg J$, La_2CuO_4 is expected to cross from the RC regime to the quantum critical (QC) regime. In this phase, typical of 2D quantum systems, the only energy scale is set by temperature so that the dynamical critical exponent z is $z=1$ and $\xi_{2D}\simeq aJ/T$.

The comprehension of the experimental findings in the paramagnetic phase of La_2CuO_4 is still not well established. From ^{63}Cu NQR T_1 and T_2 measurements Imai *et al.*[5] concluded that the relaxation rate is in agreement with the theoretical calculations based on the dynamical scaling for $S=1/2$ 2D-QHAF.[3] These results were used to claim the occurence of the QC regime[6,7] and furthermore to argue[8] that the disorder related to hole doping extends the QC regime to lower temperatures. On the other hand, neutron scattering data,[9] combined with Monte Carlo simulations, in the best 2D-QHAF (namely $Sr_2CuO_2Cl_2$) and more recently[10] also in La_2CuO_4 showed no evidence of crossover from the RC to the QC regime.

The early Cu NQR data[5] have been subsequently reexamined by Matsumura *et al.*[11] which concluded that the deviation of the relaxation rate from the prediction expected in the RC regime was not associated to the crossover to the QC regime. A detailed comparison of the data for ^{63}Cu T_1 and spin echo decay rate in La_2CuO_4 with theoretical predictions based on quantum Monte Carlo and maximum entropy analytic continuation, has recently been given,[12] again raising doubts on the existence of a temperature regime where QC scaling expressions can be applied.

In this paper we report ^{63}Cu NQR relaxation measurements carried out in La_2CuO_4 doped with Zn, aiming at investigating the effect of the disorder associated to the Zn^{2+} $S=0$ for Cu^{2+} $S=1/2$ substitution on ξ_{2D}. The ^{63}Cu NQR relaxation is driven by the correlated spin dynamics of the Cu^{2+} magnetic moments and the spin-lattice relaxation rate $2W=1/T_1$ and the spin echo decay rate $1/T_{2G}$

can be directly related to ξ_{2D} on the basis of scaling arguments. It is first shown that the NQR quantities in pure La_2CuO_4, in the temperature range $450 \lesssim T \lesssim 900$ K, quantitatively follow the behavior expected for the RC regime with a dynamical scaling exponent $z=1$. Thus ξ_{2D} is extracted in close form with minor use of adjustable parameters (only a numerical factor of the order of unity is introduced in order to take into account quantum corrections to the amplitude of spin fluctuations). The data are in good agreement with the findings from neutron scattering.[10] Then, having established a reliable connection between Cu NQR relaxation rates and ξ_{2D}, the data in the doped system $La_2Cu_{1-x}Zn_xO_4$ for $x=0.025, 0.08$, and 0.11 are used to derive $\xi_{2D}(x,T)$. An analogous derivation, of less quantitative value, can be obtained by analyzing the x dependence of the Néel temperature $T_N(x)$ in $La_2Cu_{1-x}Zn_xO_4$, as already discussed in a previous work[13] based on ^{139}La NQR and μSR in the AF phases. The effect of Zn on ξ_{2D} turns out to be rather well justified from the changes on the spin stiffness expected from the dilution of the magnetic spins. No evidence of a dramatic increase in quantum fluctuations or of a crossover to the quantum disordered regime is found.

The paper is organized as follows. In Sec. II information on experimental aspects, some basic equations, and the experimental results are presented. In Sec. III the ^{63}Cu NQR relaxation rates are related to the Cu^{2+} spin dynamics. First the classical limiting condition ($T \gg J$) is considered, pointing out that even at the highest temperatures the correspondent theoretical expressions for $1/T_1$ and $1/T_{2G}$ can hardly be used. The regime of strong 2D correlation is then discussed and the appropriate relationships for ξ_{2D} are worked out. Then $\xi_{2D}(x,T)$ is derived and discussed in terms of Zn-induced modifications on the spin wave stiffness. Comparison with the case of hole doping is discussed, also in view of the much stronger suppression of the spectral weight of the spin excitations at low frequencies in La_2CuO_4 doped with itinerant holes. Finally in Sec. IV summarizing remarks and conclusions are given.

II. EXPERIMENTALS AND EXPERIMENTAL RESULTS

The powders of $La_2Cu_{1-x}Zn_xO_4$ and the pure La_2CuO_4 used as reference have been prepared by Licci and Raffo (MASPEC, Parma, Italy) (Ref. 13) by conventional solid state reactions in air, starting from La_2O_3, CuO, and ZnO (purity $>99.99\%$). The pellets have been annealed for 24–48 h at 1050 °C. The treatment was repeated three or four times at temperatures around 1050 °C with intermediate room temperature grinding and check of the x-ray diffraction pattern. No evidence of spurious phases or of segregation was obtained by this technique. Thus the doping amount x was simply estimated from the stoichiometric ratios of the starting compounds. In order to fully oxydize the products, annealing in oxygen at 480–500°C was first performed for 150–200 h. For the NQR experiments the samples have been ground again and the excess oxygen, which is known to modify the magnetic properties, has been removed either with zirconia getters or by annealing in N_2 atmosphere at 700°C for 24 h. To prevent further oxygen exchange during the measurements the powders have been sealed in Pyrex ampoules. Since Pyrex becomes porous at high temperatures, the ampoule was kept in N_2 atmosphere.

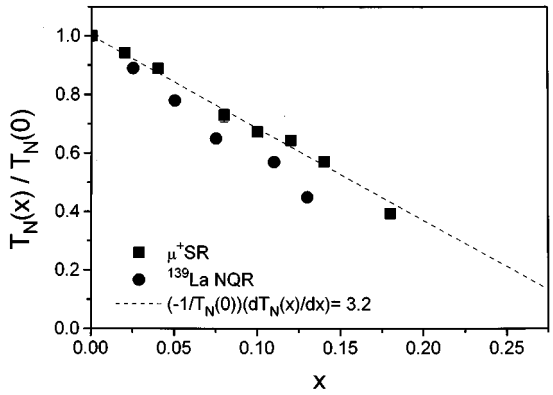

FIG. 1. Néel temperatures $T_N(x)$ in the samples of $La_2Cu_{1-x}Zn_xO_4$ used in the present work, as obtained from ^{139}La NQR spectra and μSR precessional frequencies. For $x=0$ we found $T_N=315\pm2$ K.

The transition temperatures from the AF to the PA phases have been monitored through the ^{139}La NQR spectra and from the extrapolation to zero of the zero-field μSR precessional frequencies (see Ref. 13 for details). The Néel temperature for the pure La_2CuO_4 turned out $T_N(0)=315\pm2$ K. The x dependence of T_N is reported in Fig. 1. It is noted that T_N is slightly affected by Zn doping and the absolute values of $T_N(x)$ are the highest reported in literature (see Ref. 13 and references therein). This demonstrates that the oxygen stoichiometry is close to the ideal one. The temperature control in the measurements presented in the following was such that for the highest temperature the uncertainty was kept within ±1 K during the full time of the measure (up to 6–8 h for a full recovery plot in NQR ^{63}Cu spin-lattice relaxation).

The ^{63}Cu relaxation rates have been obtained with standard pulse techniques. T_1 was deduced from the recovery of the echo amplitude after a sequence of saturating pulses yielding equalization in the populations of the $\pm1/2$ and $\pm3/2$ ^{63}Cu NQR levels. For the samples at large doping ($x \geqslant 0.08$) the NQR lines are very broad [see Fig. 2(a)] and some evidence of a small contribution from spectral diffusion was detected at short times of the recovery. In these cases only the exponential part of the recovery $y(t) = \exp\{-6Wt\}$ was used to extract the relaxation rate $1/T_1 = 2W$. It can be noticed that the ^{63}Cu NQR line in doped samples is asymmetric and a component, more evident for $x=0.025$, appears around $\nu_Q=32.4$ MHz [see Fig. 2(a)]. This shoulder might be due to the nuclei which are nearest neighbors to Zn impurities. T_1 measurements carried out by irradiating at the frequency of the shoulder showed nonexponential recovery at short times and a slightly longer T_1, consistent with the aforementioned hypothesis. The relaxation measurements that we are going to report refer to irradiation of the center of the line and therefore to nuclei which are not nearest neighbors (NN) to the Zn impurities. In Fig. 2(b) a typical recovery plot up to the second decade is shown. As in most systems with disorder, some deviations from the exponential behavior are present at long times. The deviations in the second decade are likely to be related to the

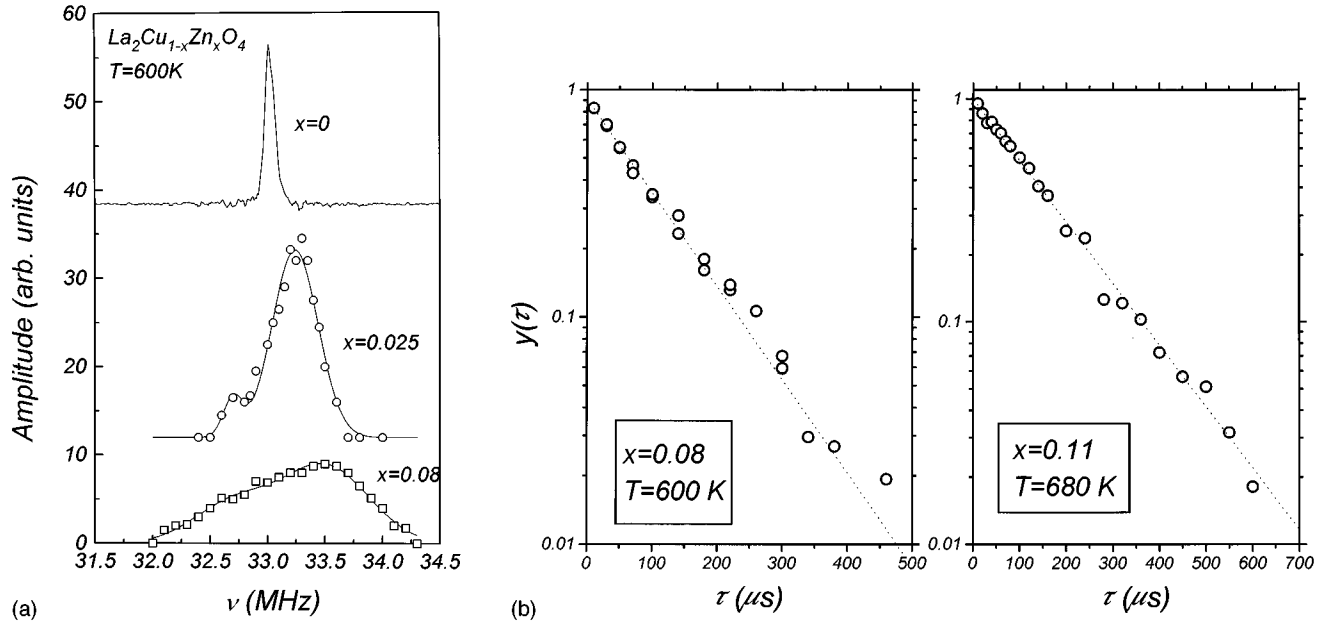

FIG. 2. (a) Typical ^{63}Cu NQR spectra in $La_2Cu_{1-x}Zn_xO_4$. In the pure sample the line was obtained through direct Fourier transformation of half of the echo signal. For $x\neq 0$ the spectra were reconstructed by sweeping the irradiation frequency $\nu_{\rm irr}$, Fourier transforming half of the echo signal and reporting the amplitude read at $\nu_{\rm irr}$. (b) A typical recovery law for the amplitude of the echo signal after saturation is shown, for the sample with $x=0.08$ ($T=600$ K) and for the sample with $x=0.11$ ($T=680$ K). For $x=0.08$, from the fit of the points in the first decade one derives $2W=3.1\pm 0.07$ ms^{-1}, while by fitting the data in the two decades one has $2W=3.19\pm 0.09$ ms^{-1}. For the $x=0.11$ sample the fitting of the data over two decades gives $2W=2.21\pm 0.06$ ms^{-1}.

Cu nuclei nearest neighbors of Zn impurities which have longer T_1's. However, they little affect the evaluation of the relaxation rate for the nuclei in the bulk of the sample, as pointed out in the caption to Fig. 2(b). One could observe that the deviations from the exponential behavior occuring in the second decade in $La_2Cu_{1-x}Zn_xO_4$ are less marked than the ones in Zn-doped $YBa_2Cu_3O_{7-\delta}$.[14] This difference is most likely due to the fact that the ^{63}Cu nuclei nearest neighbour to Zn in $La_2Cu_{1-x}Zn_xO_4$ has a resonance sizably shifted from the one for the nuclei in the bulk.

The Gaussian part of the spin echo decay was obtained from the plot of the echo amplitude $h(2\tau)$ as a function of the delay τ between the two rf pulses. The behavior[15]

$$h(2\tau)=h(0)e^{\{-5.6\cdot 2\tau/T_1\}}e^{\{-(2\tau)^2/2T_{2G}^2\}} \qquad (2)$$

was found to be very well verified and $1/T_{2G}$ was thus extracted (Fig. 4). One can observe that the slight modification, upon Zn doping, expected in the anisotropy ratio of the hyperfine Hamiltonian (see Sec. III A) modifies the numerical factor in the Lorentzian part of Eq. (2) only by a few percent, for the maximum amount of doping. In the following we will neglect this correction. The length of the pulses maximizing the echo signal was noticed to change slightly according to the width of the NQR line, in qualitative agreement with the calculations by Man.[16] It should be remarked that a correct evaluation of T_{2G} is possible only when the line is narrow enough so that a complete irradiation by the RF pulse is achieved. This is the case for pure La_2CuO_4 or for moderately Zn-doped compounds. The strength of the RF field was estimated around 100 G. With a typical pulse length of $\simeq 3\mu$s the ^{63}Cu NQR line was fully irradiated only for relatively narrow lines, i.e., $x\leqslant 0.025$. No modification in the absolute values of T_{2G} was observed on reducing the RF power. However, for $x\geqslant 0.08$ the NQR line is dominated by the inhomogeneous broadening due to disordering and thus the meaning of $1/T_{2G}$ derivation is doubtful, although the Gaussian behavior was always well verified.

III. RELAXATION RATES, SPIN DYNAMICS, AND CORRELATION LENGTH

In this section we relate the ^{63}Cu NQR spin-lattice relaxation rate and the echo dephasing time to the correlated Cu^{2+} spin dynamics and to the in-plane correlation length ξ_{2D}. For convenience we first consider the limit of infinite temperature. In the regime of strong correlation, namely for $T<J$, we use scaling arguments to derive the relationships of T_1 and of T_{2G} to ξ_{2D}. Then the theoretical expressions for ξ_{2D} suggested by recent theories for 2D-QHAF are considered and the role of the disorder due to Zn doping is addressed.

A. Infinite temperature approximation

In the high temperature limit the correlation among the Cu^{2+} spins can be neglected. We will consider the magnetic relaxation process of ^{63}Cu as driven by the interaction with the on-site Cu^{2+} spin and with the four nearest neighbor (NN) ones. For the electron-nucleus Hamiltonian we refer to the well-established Mila-Rice form.[17] Thus the field at the nuclear site $\vec{h}$ is written

$$\vec{h}=A\vec{S}_o+\sum_{i=1}^{4} B\vec{S}_i\,. \qquad (3)$$

Then from the expression

$$\frac{1}{T_1}=2W=\frac{\gamma^2}{2}\int_{-\infty}^{+\infty}\langle h_+(0)h_-(t)\rangle e^{-i\omega_Q t}dt \tag{4}$$

by considering the correlation function for the transverse (i.e., in the ab plane) components of the spin operators $\vec{S}$ in the usual Gaussian form,[18] with an effective correlation time related to the inverse of the corrected[5] Heisenberg exchange frequency ω_e, where

$$\omega_e=\left[\left(\frac{2J^2k_B^2zS(S+1)}{3\hbar^2}\right)\left(\frac{1-2A_\perp B}{A_\perp^2+4B^2}\right)\right]^{1/2} \tag{5}$$

with z the number of NN spins and where the correction pertinent to the transferred hyperfine interaction B in the NN spin correlation function has been taken into account, one derives

$$\left(\frac{1}{T_1}\right)_\infty=\frac{1}{4}\gamma^2(A_\perp^2+4B^2)\frac{\sqrt{2\pi}}{\omega_e}. \tag{6}$$

In the above equation one can use $A_\perp=80$ kG and $B=83$ kG (corresponding to 40 kOe/μ_B and 41.5 kOe/μ_B, respectively). Then from Eq. (5) one estimates the high temperature limit of the relaxation rate: $(1/T_1)_\infty=4.4\times10^3$ s^{-1}. This value is about twice that of the experimental result at $T\simeq900$ K, where $1/T_1=2.6\times10^3$ s^{-1}. The difference is likely to reflect the correlation effects in the spin fluctuations, as is discussed in the following subsection [see the caption in Fig. 3(a)].

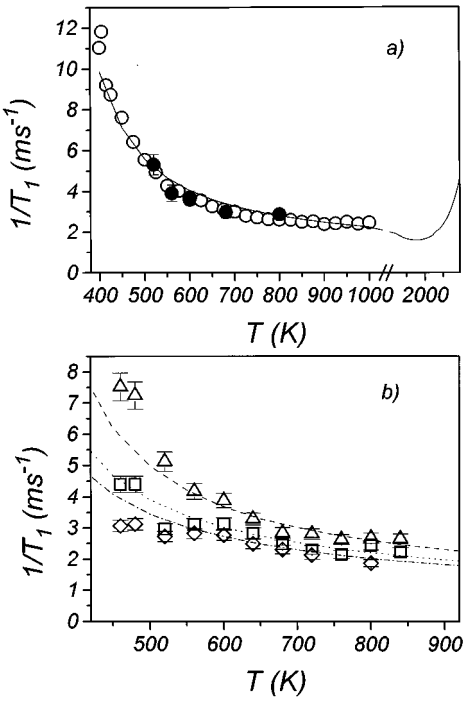

FIG. 3. (a) ^{63}Cu NQR relaxation rates in the paramagnetic phase of La_2CuO_4 (○ representative points from Ref. 11, ● data from this work). The solid line gives the theoretical form for $2W$ as obtained from Eq. (10) in the text by means of a numerical integration and in the assumption of $\xi_{2D}(T)$ described by Eq. (1). The increase of $1/T_1$ for $T\geqslant1800$ K is due to the fact that when $\xi\leqslant1$ the $\mathcal{A}_{\vec{q}}$ form factor enhances the contribution to the relaxation rate related to the long wavelength excitations for which $\mathcal{A}_{\vec{q}}$ takes the maximum value $\mathcal{A}_{\vec{q}}=(A_\perp+4B)^2$, which instead is filtered out for $\xi\gg1$. (b) ^{63}Cu NQR relaxation rates in $La_2Cu_{1-x}Zn_xO_4$ for $x=0.025$ (△), $x=0.08$ (□) and $x=0.11$ (◇). The dashed, dotted, and dot-dashed lines show the respective behavior expected according to the dilution model.

B. Regime of strong 2D correlation

For $T\leqslant J$, with ξ_{2D} at least of the order of some lattice units, the Cu^{2+} spin fluctuations become correlated. From Eq. (3), by introducing in Eq. (4) the collective spin components and their decay rate $\Gamma_{\vec{q}}$ (with $\Gamma_{\vec{q}}\gg\omega_Q$) one obtains

$$\frac{1}{T_1}=\frac{\gamma^2}{2}\frac{1}{N}\sum_{\vec{q}}(2|S_{\vec{q}}|^2/\Gamma_{\vec{q}})\times\{A_\perp-2B[\cos(q_xa)+\cos(q_yb)]\}^2 \tag{7}$$

where the 2D wave vector $\vec{q}$ starts from $q_{AF}=(\pi/a,\pi/a)$. By resorting to conventional scaling arguments[19] one can write

$$|S_{\vec{q}}^\alpha|^2=|S_{q_{AF}}^\alpha|^2f(q\xi)=\epsilon\frac{S(S+1)}{3}\left(\frac{\xi}{a}\right)^{2-\eta}f(q\xi), \tag{8a}$$

$$\Gamma_{\vec{q}}=\Gamma_{q_{AF}}g(q\xi)=(2\omega_e/\sqrt{2\pi})\left(\frac{\xi}{a}\right)^{-z}g(q\xi), \tag{8b}$$

where $\xi\equiv\xi_{2D}$, η is expected to be negligible [$\eta\simeq0.028$ (Ref. 20)], $\alpha=x,y,z$, while the dynamical scaling exponent z depends on the properties of the spin dynamics. In Eq. (8a) ϵ is a constant of order of unity which accounts for the reduction of the amplitude of spin fluctuations due to quantum effects. Moreover, in Eq. (8b) a proper match has been achieved with the Heisenberg exchange frequency ω_e which describes the uncorrelated spin fluctuations in the limit of infinite temperature. For the scaling functions f and g in Eqs. (8) we will assume the simple MFA forms

$$f(q\xi)=\frac{\beta}{q^2\xi^2+1}=g(q\xi)^{-1}, \tag{9}$$

where $1/\beta=(\xi^2/4\pi^2)\int d\vec{q}/(1+q^2\xi^2)$ is a normalization factor which preserves the sum rule $\Sigma_{\vec{q}}|S_{\vec{q}}^\alpha|^2=\epsilon NS(S+1)/3$. Then from Eqs. (7) and (8) one has

$$\frac{1}{T_1}=\gamma^2\frac{S(S+1)}{3}\epsilon\left(\frac{\xi}{a}\right)^{z+2}\frac{\beta^2\sqrt{2\pi}}{\omega_e}\left(\frac{a^2}{4\pi^2}\right)\int_{BZ}d\vec{q}\,\frac{\{A_\perp-2B[\cos(q_xa)+\cos(q_yb)]\}^2}{(1+q^2\xi^2)^2}. \tag{10}$$

In order to test quantitatively the validity of the assumptions underlying the derivation of Eq. (10) we performed an estimate of the theoretical expression for the relaxation rate by means of a numerical integration over the Brillouin zone (BZ) and by using for the temperature dependence of ξ the form in Eq. (1), with the value $z=1$ for the dynamical scaling exponent and $J=1588$ K.[10] The result of this evaluation for $1/T_1$ is reported in Fig. 3 (solid line). One notes that for $\epsilon=0.3$ (which is of the correct order of magnitude[3]) the agreement with the experimental results is good either for the absolute value as well as for the temperature dependence.

A simple analytical form which emphasizes the connection of $1/T_1$ to ξ_{2D} can be obtained if an average (over the BZ) form factor

$$\langle \mathcal{A}_{\vec{q}} \rangle = \langle \{A_\perp - 2B[\cos(q_x a)+\cos(q_y b)]\}^2 \rangle_{\mathrm{BZ}} = A_\perp^2 + 4B^2$$

is taken out from the integration in Eq. (10). Then the relaxation rate can be written

$$\frac{1}{T_1} \simeq \gamma^2 \frac{\epsilon S(S+1)}{3} \frac{\sqrt{2\pi}}{\omega_e} \frac{\pi}{[\ln(q_m \xi)]^2} \langle \mathcal{A}_{\vec{q}} \rangle \left(\frac{\xi}{a}\right)^z \simeq \frac{4.2\times 10^3}{[\ln(q_m \xi)]^2} \left(\frac{\xi}{a}\right)^z, \tag{11}$$

where $q_m = 2\sqrt{\pi}/a$, the integration having been carried out over a circle centered around q_{AF}. To give an idea, the assumptions leading to Eq. (11), for instance, at $T \simeq 1000$ K, imply a relaxation rate $1/T_1 \simeq 2.2\times 10^3$ s^{-1} instead of the value $1/T_1 \simeq 2.6\times 10^3$ s^{-1} numerically obtained from Eq. (10) [see solid line in Eq. (2)]. One can remark that the other two assumptions for the form factor $A_{\vec{q}}$, namely $A_\perp^2 + 4B^2$ (totally uncorrelated fluctuations) or $(A_\perp - 4B)^2$ (for complete AF correlation) are expected to hold only for $T \geqslant 1500$ K or for $T \ll J$, respectively (see comment in the caption to Fig. 3). In summary, although $1/T_1$ is nearly proportional to ξ_{2D}, non-negligible corrections, associated to the q dependence of the form factor, have to be taken into account in order to extract quantitative values of ξ_{2D}.

As regards the Gaussian component of the spin echo decay rate, it has been shown that the dominant contribution arises from the indirect nuclear spin-spin coupling.[15] Then one can write[21]

$$\left(\frac{1}{T_{2G}}\right)^2 = \frac{0.69}{4}\hbar^2\gamma^4 \left\{ \frac{1}{N}\sum_{\vec{q}} C_{\vec{q}}^4 \chi'^2(\vec{q},0) - \left(\frac{1}{N}\sum_{\vec{q}} C_{\vec{q}}^2 \chi'(\vec{q},0) \right)^2 \right\}, \tag{12}$$

where $C_{\vec{q}} = A_\parallel - 2B[\cos(q_x a)+\cos(q_y b)]$ ($A_\parallel = -332$ kG). By using the same scaling arguments outlined for T_1 and since $|S_{\vec{q}}^\alpha|^2 = k_B T \chi^{\alpha\alpha}(\vec{q},0)$, one has

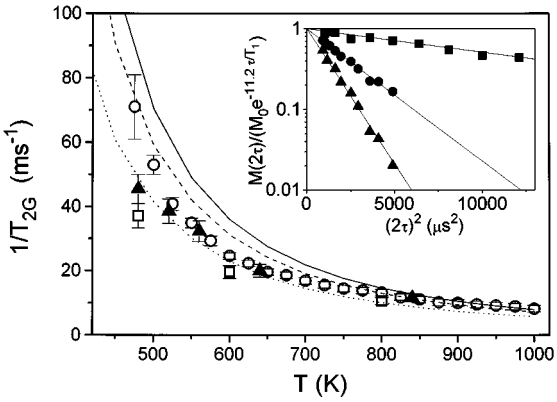

FIG. 4. Gaussian component $1/T_{2G}$ of the ^{63}Cu NQR spin echo decay rate as obtained from the dephasing time of the echo according to Eq. (2) in the text, as a function of temperature for $x=0$ (circles, representative points from Ref. 11), $x=0.025$ (triangles), and $x=0.08$ (squares). The solid, dashed, and dotted lines give the behavior according to Eq. (13), in the framework of the dilution model, for $x=0$, $x=0.025$, and $x=0.08$, respectively. In the inset is shown how Eq. (2) is well obeyed, at $T=560$ (triangles), 640 (circles), and 840 K (squares), for $x=0.025$. In view of the uncertainty in the definition of T_{2G} for large doping (see text) the results for $x=0.08$ are shown only at the sake of comparison.

$$\left(\frac{1}{T_{2G}}\right)^2 = \frac{0.69\hbar^2\gamma^4}{4(k_B T)^2} \left(\frac{\epsilon S(S+1)}{3}\right)^2 \beta^2 \left(\frac{\xi}{a}\right)^4 \times \left\{ \frac{a^2}{4\pi^2}\int_{\mathrm{BZ}} d\vec{q} \frac{C_{\vec{q}}^4}{(1+q^2\xi^2)^2} - \left(\frac{a^2}{4\pi^2}\int_{\mathrm{BZ}} d\vec{q} \frac{C_{\vec{q}}^2}{1+q^2\xi^2} \right)^2 \right\}. \tag{13}$$

By using for ξ_{2D} the form given in Eq. (1) and adding the second moment from the direct spin-spin coupling $[(1/T_{2G})_{\mathrm{dir}}^2 = (4.5\times 10^3)^2$ s^{-2} (Ref. 22)], again a reasonable agreement with the experimental results is found (Fig. 4).

If an average form factor is taken out of the integral as for T_1 [see Eq. (11)] then Eq. (13) becomes

$$\left(\frac{1}{T_{2G}}\right)^2 \sim \frac{1}{T^2} \left\{ \langle C_{\vec{q}}^4 \rangle \left(\frac{\xi}{a}\right)^2 - (\langle C_{\vec{q}}^2 \rangle)^2 \right\}, \tag{14}$$

implying that for $(\xi_{2D}/a) \gg 1$, $1/T_{2G} \sim \xi/T$. Then in light of Eq. (11),

$$\frac{T_1 T}{T_{2G}} \sim \xi^{1-z} \sim \text{const.} \tag{15}$$

for $z=1$.

It can be noted that Eqs. (11), (14), and (15) are slightly different from the ones in Ref. 6, where $\chi(\vec{q},\omega)$ was scaled in the form $\chi(\vec{q},\omega) = \xi^2 F(q\xi, \omega/\omega_e)$. The difference is due to the fact that, in terms of $\chi(\vec{q},\omega)$, our scaling relations are equivalent to include the single-particle susceptibility $\chi_0 \sim 1/T$ (see note in Ref. 19). Thus our derivation does not imply the assumption $\xi(2\pi T_s)=1$ used in Ref. 3.

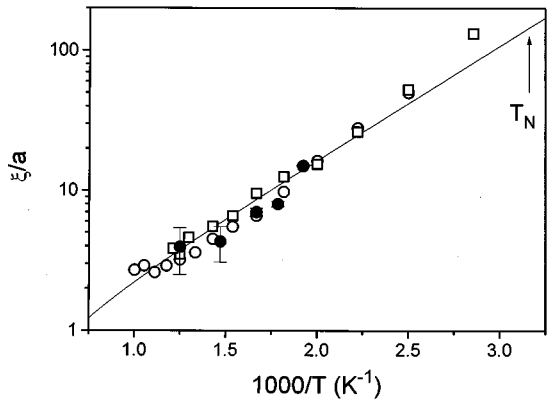

FIG. 5. In-plane magnetic correlation length as a function of temperature in the paramagnetic phase of pure La_2CuO_4, as extracted from ^{63}Cu NQR spin-lattice relaxation rate as explained in the text (● our data, ○ data from Ref. 11). For comparison some representative results from neutron scattering (Ref. 10) are also shown (□).

The scaling relations given in Eqs. (8a) and (8b) should be modified when the strength of quantum fluctuations becomes important.[20] If scaling appropriate for the QC regime is used, namely $|S_{\vec{q}}|^2=\xi h(q\xi)$,[20] following the same procedure outlined above one would derive

$$\left(\frac{1}{T_1}\right)_{\mathrm{QC}} \sim \text{const}, \tag{16a}$$

$$\left(\frac{1}{T_{2G}}\right)^2_{\mathrm{QC}} \sim \frac{1}{T^2}\left\{\langle C^4_{\vec{q}}\rangle - \left(\frac{\langle C^2_{\vec{q}}\rangle}{\xi}\right)^2\right\}. \tag{16b}$$

It can be observed that in the strong correlation limit, $\xi_{2D}\gg 1$, the ratio T_1T/T_{2G}, depending on the dynamical exponent z, is still constant for $z=1$, as in Eq. (15). We would like to remark that Eq. (16a) implies that the independence of the relaxation rate on Sr doping and temperature observed in $La_{2-x}Sr_xCuO_4$ (Ref. 5) is an indication that charge doping drives La_2CuO_4 to the QC regime. This is at variance with the effect of Zn doping, as we are going to show in the following.

C. Temperature dependence of ξ_{2D}: Effect of Zn-induced disorder

Having related ^{63}Cu NQR T_1 and T_{2G} to the in-plane correlation length, now we are going to analyze the temperature dependence of $\xi_{2D}(x,T)$ extracted from our data, by discussing the role of the disorder due to Zn doping in $La_2Cu_{1-x}Zn_xO_4$.

In Fig. 5 the correlation length, derived from ^{63}Cu NQR T_1 for pure La_2CuO_4 following the procedure outlined in Sec. III B [see Eq. (10)], is reported. For comparison some representative results from neutron scattering are shown. In all the temperature range the results from the two techniques are in good agreement, even quantitatively. The temperature behavior of ξ_{2D} is rather close to the one theoretically predicted for the RC regime, at least for $T\lesssim 900$ K. One could

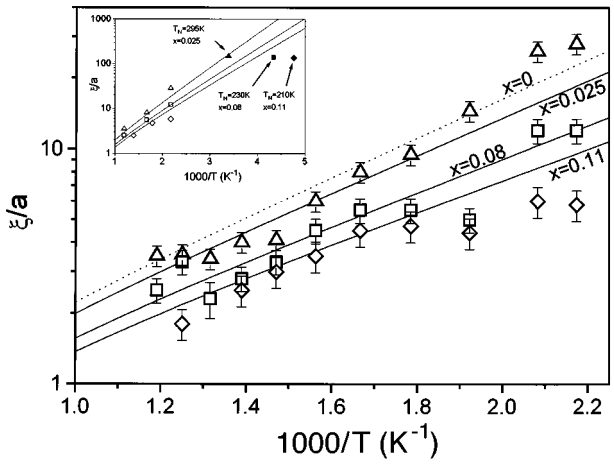

FIG. 6. Temperature dependence of the correlation length in Zn-doped La_2CuO_4, as obtained from the experimental results shown in Fig. 3(b) on the basis of Eq. (10), modified in order to take into account the spin vacancy (see text). The solid lines represent the behavior for ξ_{2D} expected on the basis of the dilution model, as given by Eq. (20) in the text. The inset shows the extrapolation of ξ_{2D} as derived from Eq. (20) (solid lines) and the comparison with the values of $\xi_{2D}(x,T_N)$ as obtained from the x dependence of T_N [Eq. (18) in the text].

observe that the expression for ξ_{2D} derived in Ref. 3 differs from the one given in Eq. (1) and from the experimental values by a factor $\simeq 1.6$, which originates from the assumption $\xi(2\pi\rho_s)=1$.[3]

The occurrence of a QC regime with $\xi_{2D}\sim 1/T$ and $1/T_1$ nearly constant [see Eqs. (16)] is possibly observed only for $T\gtrsim 900$ K. This implies that in a large temperature range above T_N La_2CuO_4 is in the RC regime and the strength of quantum fluctuations is small.

The overall consistency of the theoretical picture encourages one in using it in order to derive $\xi_{2D}(x,T)$ from the ^{63}Cu NQR T_1 in Zn-doped samples. At this purpose one has to correct Eq. (10) in order to take into account that the probability of having a Cu^{2+} nearest neighbor is reduced by a factor $(1-x)$. Then $\mathcal{A}_{\vec{q}}=(A_\perp-2(1-x)B[\cos(q_xa)+\cos(q_yb)])^2$ and $J(x)=J(0)(1-x)^2$. Therefore, from Eq. (5) one has $\omega_e(x)=\omega_e(0)(1-x)^2$, and in the high temperature limit

$$T_1(x)=\frac{(1-x)^2(A_\perp^2+4B^2)}{A_\perp^2+4(1-x)B^2}T_1(0). \tag{17}$$

Thus in a description based on the simple dilution model one should find $1/T_1$ increasing with x. Experimentally one finds an opposite trend (see Fig. 3). This is consistent with a decrease in the correlation, already present at $T\simeq 900$ K, with Zn doping.

The results for $\xi_{2D}(x,T)$ extracted from the experimental data in Fig. 2, according to Eq. (10) modified to take into account Zn substitution, are reported in Fig. 6.

Another way to analyze the effect of Zn on ξ_{2D} is to consider the x dependence of T_N (Fig. 1). In fact, by includ-

ing the substitutional effect on the interplane interaction $J_\perp(x)$ within the dilution model, the 3D ordering temperature for 2D-HAF can be written $T_N = J_\perp(0)\ (1-x)^2\xi^2(x,T_N)$. Then from the data in Fig. 1 one can derive[13]

$$\xi(x,T_N) = \xi(0,T_N)\frac{(1-3.2x)^{1/2}}{1-x}. \tag{18}$$

To discuss our findings about the role of Zn in reducing ξ_{2D}, let us consider first the effect on the spin stiffness $\rho_s = c_{sw}^2\chi_\perp(0)$. In the low concentration limit, for a square lattice[23]

$$\rho_s(x) = \rho_s(0)[1-(2-x)x] \tag{19}$$

that according to Eq. (1), for $T \ll J$, implies

$$\xi(x,T) = \xi(0,T)e^{\{-x(2-x)1.15J/T\}}. \tag{20}$$

In Fig. 6 the behavior expected on the basis of Eq. (20) is compared to the data derived from ^{63}Cu NQR $1/T_1$. A satisfactory agreement is observed.

Another possibility to take into account in discussing the decrease of the relaxation rate upon Zn doping in principle is the crossover to the QC regime due to the decrease in the spin stiffness. As it has been discussed in Sec. III B, in pure La_2CuO_4 the crossover from RC to QC regime could occur only at $T_c \gtrsim 900$ K. From the data in Fig. 3, and in the light of Eqs. (16), one can note that Zn doping could possibly push the system in the QC regime only above $T \simeq 700$ K, and for $x \gtrsim 0.11$.

The reduction in $1/T_1$ observed at low temperatures, again in principle, could be associated to a spin gap opening at $T^\star \simeq 500-600$ K, similarly to the case of itinerant defects.[24,25] Then one would expect a suppression of the spectral weight for frequencies lower than $c_{sw}/\xi(T^\star)$. This does not seem the case in $La_2Cu_{1-x}Zn_xO_4$. In fact, as a consequence of the spin-gap opening one would expect T_{2G} to become temperature independent, while we have observed a progressive increase of $1/T_{2G}$ on cooling, with disappearing of the echo signal. Furthermore, the eventual quenching of the increase of $\xi_{2D}(x)$ on cooling is not consistent with the relatively high Néel temperatures $T_N(x)$. Anyway, if the spin-gap opening is associated to a quantum disordered regime[25,20] it cannot take place in $La_2Cu_{1-x}Zn_xO_4$, where quantum fluctuations do not appear significant.

It is important to remark that the effect of Zn doping on ξ_{2D} deduced from our measurements is somewhat at variance with the one observed on the relaxation rate upon charge doping. In $La_{1.96}Sr_{0.04}CuO_4$ a reduction by a factor 3 is induced in $1/T_1$ at $T \simeq 450$ K, while the same effect requires a Zn doping around $x \gtrsim 0.11$. The stronger effect of charge doping could be attributed to the range of the perturbation and to the itinerancy[26] of the singlet in some respects equivalent to a spin vacancy. The counterpart of the sizable effectiveness on ξ_{2D} of charge doping is the drop of the Néel temperature. While for Zn doping one has a linear decrease of $T_N(x)$ (Fig. 1), with initial suppression rate $(1/T_N)\lim_{x\to 0}[dT_N(x)/dx] \simeq -3.2$, in $La_{2-x}Sr_xCuO_4$ one has a nonlinear reduction of T_N, with a marked drop for $x \simeq 0.02$. It is conceivable that the nature of the disorder induced in the AF matrix by itinerant defects is different from the one due to localized defects. In the former case, for instance, the charge correlations can induce the formation of walls of itinerant holes which are pinned for particular doping levels[27] and cause an enhancment of quantum fluctuations which instead are negligible for Zn-doped La_2CuO_4.

IV. SUMMARIZING REMARKS AND CONCLUSIONS

The correlated $S = 1/2$ Cu^{2+} spin dynamics in the paramagnetic phase of the 2D-QHAF La_2CuO_4 and the effect of Zn^{2+} $S = 0$ for Cu^{2+} substitution has been studied through ^{63}Cu NQR relaxation times T_1 and T_{2G}. First the problem of suitable relationships of the correlated spin dynamics with the NQR quantities has been addressed. By using scaling arguments the relaxation rate $1/T_1$ has been related to the spin fluctuation frequency Γ_{AF} at the antiferromagnetic wave vector $q_{AF} = (\pi/a, \pi/a)$ through the in-plane magnetic correlation length ξ_{2D}. Γ_{AF} has been written $\Gamma_{AF} = 2\omega_e(\xi_{2D}/a)^{-z}/\sqrt{2\pi}$, with z the dynamical critical exponent. The Gaussian part of the echo dephasing rate $1/T_{2G}$ has also been related to the q-integrated static generalized susceptibility and then to ξ_{2D}. It has been shown that the absolute values and the temperature dependence of $1/T_1$ and $1/T_{2G}$ are well described by the theoretical expressions derived in the framework of the aforementioned approach. In particular, for $T \lesssim 900$ K $\xi_{2D}(T)$ follows a temperature dependence of the form expected for a 2D-QHAF in the RC regime and consistency with recent neutron scattering data in La_2CuO_4 has been obtained.

On the basis of the established connections of T_1 and of T_{2G} to the correlation length, the ^{63}Cu NQR relaxation rates have been used to study the effects on $\xi_{2D}(x,T)$ of Zn doping in the PA phase of $La_2Cu_{1-x}Zn_xO_4$. The results obtained for x up to 11% have been interpreted in terms of the reduction of the spin stiffness $\rho_s = c_{sw}^2\chi_\perp(0)$. By including the substitutional effects in the framework of conventional dilutionlike models, the expression $\rho_s(x) = \rho_s(0)[1-x(2-x)]$ for square lattices in the low concentration limit has been shown to describe rather well the temperature and x dependences of ξ_{2D}. A similar conclusion is also obtained from the Zn dependence of the Néel temperature $T_N(x)$ for $\xi_{2D}(x,T_N)$, having included the dilution model for the interplane interaction. Thus one is led to the conclusions that for $T \lesssim 700$ K the Zn doping leaves the 2D-QHAF La_2CuO_4 in the RC regime and that the x and T dependence of ξ_{2D} is accounted for by a simple dilutionlike effects on the spin stiffness, without a remarkable enhancement of quantum fluctuations, as it occurs instead for hole-doped La_2CuO_4.

ACKNOWLEDGMENTS

We would like to thank S. Aldrovandi for his technical assistance in setting up the high temperature radio-frequency probe and F. Raffa for his help in carrying out some of the μSR measurements. Useful discussions with M. Acquarone, F. Borsa, and V. Tognetti are gratefully acknowledged. The research was carried out with the financial support of INFN (Istituto Nazionale di Fisica Nucleare) of INFM (Istituto Nazionale di Fisica della Materia).

[1] For a concise overview, see M. Greven *et al.*, Z. Phys. B **96**, 465 (1995).
[2] See B. Keimer *et al.*, Phys. Rev. B **46**, 14 034 (1992), and references therein.
[3] S. Chakravarty, B. I. Halperin, and D. R. Nelson, Phys. Rev. B **39**, 2344 (1989); S. Tyc, B. I. Halperin, and S. Chakravarty, Phys. Rev. Lett. **62**, 85 (1989).
[4] P. Hasenfratz and F. Niedermayer, Phys. Lett. B **268**, 231 (1991).
[5] T. Imai *et al.*, Phys. Rev. Lett. **70**, 1002 (1993).
[6] A. Sokol and D. Pines, Phys. Rev. Lett. **71**, 2813 (1993).
[7] A. Sokol, E. Gagliano, and S. Bacci, Phys. Rev. B **47**, 14 646 (1993).
[8] A. V. Chubukov and S. Sachdev, Phys. Rev. Lett. **71**, 169 (1993).
[9] M. Greven *et al.*, Phys. Rev. Lett. **72**, 1096 (1994).
[10] R. J. Birgeneau *et al.* (unpublished).
[11] M. Matsumura *et al.*, J. Phys. Soc. Jpn. **63**, 4331 (1994).
[12] A. W. Sandvik and D. J. Scalapino, Phys. Rev. B **51**, 9403 (1995).
[13] M. Corti *et al.*, Phys. Rev. B **52**, 4226 (1995).
[14] K. Ishida *et al.*, J. Phys. Soc. Jpn. **62**, 2803 (1993).
[15] T. Imai *et al.*, Phys. Rev. Lett. **71**, 1254 (1993).
[16] P. P. Man, Phys. Rev. B **52**, 9418 (1995).
[17] F. Mila and T. M. Rice, Phys. Rev. B **40**, 11 382 (1989).
[18] T. Moriya, Progr. Theor. Phys. **16**, 641 (1956); see also the extension in Ref. 5.
[19] P. C. Hohenberg and B. I. Halperin, Rev. Mod. Phys. **49**, 435 (1977); see also Refs. 6–8 and the references therein. It is noted that the scaling conditions given in Eq. (8) in the text correspond to scale the generalized susceptibility in the form $\chi(\vec{q},\omega) = \chi_o \xi^z f(q\xi, \omega/\xi^z)$ and to use the fluctuation-dissipation theorem, with $\chi_o = S(S+1)/3k_BT$. Slightly different scaling conditions have been used in the literature (see Refs. 6–8).
[20] See A. Chubukov, S. Sachdev, and J. Ye, Phys. Rev. B **49**, 11 919 (1994), and references therein.
[21] C. H. Pennington and C. P. Slichter, Phys. Rev. Lett. **66**, 381 (1991).
[22] R. Stern *et al.*, Phys. Rev. B **51**, 15 478 (1995).
[23] See M. Acquarone and M. Paiusco, Physica C **210**, 373 (1993), and references therein.
[24] See, for instance, the special issue of Appl. Magn. Res. **3** (1992), and references therein.
[25] V. Barzykin and D. Pines, Phys. Rev. B **52**, 13 585 (1995).
[26] B. Batlogg *et al.*, Physica C **235-240**, 130 (1994); C. Y. Chen *et al.*, Phys. Rev. B **43**, 392 (1991), and references therein.
[27] J. M. Tranquada *et al.*, Nature **375**, 561 (1995); F. Borsa *et al.*, Phys. Rev. B **52**, 7334 (1995).